PAPER

Achieving multimodal locomotion by a crosslinked poly(ethylene-co-vinyl acetate)-based two-way shape memory polymer

IOP Publishing Smart Materials and Structures
Smart Mater. Struct. 31 (2022) 015034 (9pp) https://doi.org/10.1088/1361-665X/ac3c02

Achieving multimodal locomotion by a crosslinked poly(ethylene-co-vinyl acetate)-based two-way shape memory polymer

Yao Zhao[1], Kaiyuan Peng[1], Jiaxin Xi, Shima Shahab and Reza Mirzaeifar*

Department of Mechanical Engineering, Virginia Tech, Blacksburg, VA 24061, United States of America

E-mail: rmirzaei@vt.edu

Received 18 July 2021, revised 25 October 2021
Accepted for publication 22 November 2021
Published 7 December 2021

Abstract

Locomotion is a critically important topic for soft actuators and robotics, however, the locomotion applications based on two-way shape memory polymers (SMPs) have not been well explored so far. In this work, a crosslinked poly(ethylene-co-vinyl acetate) (cPEVA)-based two-way SMP is synthesized using dicumyl peroxide (DCP) as the crosslinker. The influence of the DCP concentration on the mechanical properties and the two-way shape memory properties is systematically studied. A Venus flytrap-inspired soft actuator is made by cPEVA, and it is shown that the actuator can efficiently perform gripping movements, indicating that the resultant cPEVA SMP is capable of producing large output force and recovering from large deformations. This polymer is also utilized to make a self-rolling pentagon-shaped device. It is shown that the structure will efficiently roll on a hot surface, proving the applicability of the material in making sophisticated actuators. With introducing an energy barrier, jumping can be accomplished when the stored energy is fast released. Finite element simulations are also conducted to further understand the underlying mechanisms in the complex behavior of actuators based on cPEVA SMP. This work provides critical insights in designing smart materials with external stimulus responsive programmable function for soft actuator applications.

Supplementary material for this article is available online

Keywords: two-way shape memory polymer, gripping, self-rolling, jumping, finite element analysis

(Some figures may appear in color only in the online journal)

1. Introduction

Soft actuators made by soft smart materials have attracted tremendous interests owing to their great potential for the robotic applications [1, 2]. Among different categories of smart materials, shape memory polymers (SMPs) have been extensively studied due to their extraordinary advantages, including large output forces, simple manufacturing, and low cost [3]. Although SMPs have the ability to recover to the permanent shape under external stimuli (e.g. heat, light, pH, electric field, etc), a large majority of SMPs only have irreversible shape recovery property without re-programming applied, which is also known as 'one-way shape memory effect' [4, 5]. In general, the irreversible shape memory effect of SMPs hinders their practicability for further applications.

[1] These authors contributed equally to this work.
[*] Author to whom any correspondence should be addressed.

SMPs with reversible shape memory effect (aka. two-way shape memory effect) have been recently investigated due to their shape-programmable behavior, showing a broad applicability in soft actuators and robots. The liquid crystal elastomers (LCEs) is one of the most widely used two-way SMPs because of their large deformation recovery as large as 300% [6]. For example, Ware *et al* [7] synthesized a LCE which can form complicated 3D structures upon heating and recover back to original flat shape automatically when cooled to room temperature. Shahsavan *et al* [8] fabricated a kind of light-actuated liquid crystal gels which can accomplish many complex motions, such as walking and leaping. However, the inherent low stiffness of the LCE (usually less than 1 MPa) generally becomes a serious hindrance for the soft actuators requiring high load capacity [9]. Therefore, the crosslinked poly(ethylene-co-vinyl acetate) (cPEVA)-based two-way SMP owning a relatively higher stiffness may be a promising candidate for using in soft actuators adapting to a diverse range of applications.

The PEVA are usually utilized as adhesive and structural materials due to their outstanding adhesion property [10] and remarkable mechanical properties [11]. Recently, the two-way shape memory effect of cPEVA-based polymers has been unveiled [12–14]. The mechanism of the reversible shape memory effect of cPEVA which is a kind of semi-crystalline SMPs can be attributed to the crystallization-induced elongation (CIE) and melting-induced contraction (MIC). Specifically, the semi-crystalline SMPs usually contain an amorphous phase and crystalline phases with different levels of sizes. At a relatively high temperature, the larger crystalline phase acting as a skeleton can be fixed into the first temporary shape due to well alignment stability and suitable elastic deformability. The first temporary shape is usually achieved under an external force. Upon cooling, the smaller crystalline phase can be recrystallized and oriented along the skeleton resulting in the CIE to fix the second temporary shape. When it is heated, the smaller crystalline phase will melt and shrink to the first temporary shape that is fixed by the larger crystalline phase with MIC [12–14].

Therefore, cPEVA-based polymers are attracting a great deal of attention for applications in the soft actuator domain. On the one hand, the synthesis of two-way SMPs is usually simple, which is advantageous over two-way SM composites with complex structure and fabrication techniques [15, 16]. On the other hand, the as-formed cPEVA exhibits high stiffness which enables the final systems to realize the desirable forces and torques output. Up to date, several studies have been performed on the cPEVA-based two-way SMPs. For example, cPEVA-based thin film with a well-designed pattern and reversible thermally-induced actuation has been successfully fabricated by Liu *et al* [17], which may be beneficial for the potential soft actuator miniature. Yang *et al* [18] studied the use of hierarchical chiral cPEVA fibers to fabricate artificial muscles. Hui *et al* [19] and Gao *et al* [13] also found that the different crosslinker combinations can significantly affect their two-way shape memory behavior, mechanical and thermal properties.

Locomotion is a vital topic for the soft actuators and soft robotics. The general locomotion include gripping [20, 21], walking (running, crawling, and other translational motions) [22, 23], climbing [22], swimming [21, 24], flying [25], jumping [26, 27], etc. Gripping may be the most common studied motion with different materials, actuation methods, and designing strategies. As abovementioned, one challenge for SMP grippers is that it is very difficult to achieve gripping and releasing for different cycles due to the irreversible shape memory effect, and the liquid crystal grippers can only provide small output gripping load due to low stiffness [9, 28]. Similarly, walking and other translational movements are often challenging for SMP-based actuators. For example, Chen *et al* [24] fabricated a swimming robotics which was actuated by SMP in hot water. Although the swimming robotics can swim for more than 2 s with relatively large distance, nonetheless, it cannot generate continuous movements due to the irreversible shape memory effect. Jumping becomes a more and more attractive motion for soft robotics. In order to accomplish the jumping process, an energy barrier is often needed [26, 27, 29]. For instance, Koh *et al* [26] fabricated a special bistable mechanism which was actuated by shape memory alloy (SMA). When it snapped to another state, a large energy could be released and the robotic can jump from water surface. Zhakypov *et al* [27] also fabricated a robotic which is actuated by SMA. They found that the robotic can jump from the ground when there is a fast energy release while it can only crawl when the energy is released slowly.

However, to the best of our knowledge, the cPEVA-based two-way SMPs as one kind of smart materials for various locomotion applications have not been sufficiently explored. In this work, cPEVA samples using dicumyl peroxide (DCP) as the crosslinker have been successfully fabricated. The cPEVA samples can be tailored into multiple shapes depending on the predefined ways (e.g. spiral and screw shape). More critically, some specific locomotion strategies are exhibited with cPEVA-based soft actuators, including gripping, self-rolling, and jumping. Finite element analysis is also conducted to study the related mechanism. This investigation provides critical insights in designing smart materials with high performance for a variety of advanced applications.

2. Materials and methods

The PEVA pellets with 18 wt% vinyl acetate (VA) and the DCP are purchased from Sigma-Aldrich without further treatment. Figure S1 (available online at stacks.iop.org/SMS/31/015034/mmedia) illustrates the cPEVA preparation procedure. Firstly, 2 g PEVA pellets and different amounts of DCP (2 , 4, 6, and 8 wt%) are mixed in 20 ml of toluene (anhydrous, 99.8%, Sigma-Aldrich) at 70 °C with magnetic stirring for 2 h. Then the solution is transferred into a Teflon mold, and air dried in a fume hood for about 2 d. When the toluene is fully evaporated, the bulk PEVA and DCP mixture is collected and loaded in an aluminum mold which is pre-applied with demolding agent. Finally, the cPEVA sheet sample can be obtained after curing

in a hot press (Genesis, Wabash, IN, USA) at 200 °C with 20 bar pressure for 15 min.

The mechanical properties of the cPEVA samples are measured by a dynamic mechanical analyzer (Q800 DMA, TA Instruments). The tensile tests of the samples obtained with different DCP concentrations are performed at both room temperature (i.e. 25 °C) and 70 °C. The storage and loss moduli of the sample with 6% DCP are swept from 25 °C to 85 °C at 10 Hz by dynamic mechanical analysis (DMA) test. The x-ray diffraction (XRD) profiles of the samples are measured by an x-ray diffractometer (PANalytical x'pert pro). The differential scanning calorimetry (DSC) tests of the samples are conducted using a commercial DSC unit (Q200 DSC, TA Instrument) with a heating/cooling rate 5 °C min^{-1} in running N_2.

3. Results and discussions

The influence of the crosslinker (DCP) concentration on the mechanical properties of cPEVA is firstly investigated. Figures 1(a) and (b) display the typical stress–strain curves of the cPEVA samples obtained with different DCP concentrations (2%, 4%, 6%, and 8%) at 25 °C and 70 °C, respectively. As shown in figure 1(a), all the samples have similar Young's modulus (∼15 MPa), and all the samples yield at about 2.5 MPa and 25% strain. This implies that the DCP concentration has an insignificant effect on the elasticity and yielding stress of the cPEVA. Wang *et al* [30] found that the elasticity and yielding of cPEVA are mainly determined by its crystallinity. Improving the crystallinity by increasing the content ratio of the polyethylene (PE) to VA results in the mechanical properties enhancement of cPEVA. This also means that the DCP concentration cannot significantly alter the crystal phase of cPEVA. However, it can be noted that the ultimate strains of the cPEVA samples decrease as the DCP concentration increases. For example, when the strain is larger than 350%, the 2% DCP sample does not break and is well-maintained, while the other samples are fractured (i.e. the 4% DCP sample, 6% DCP sample, and 8% DCP sample break at ∼350%, 280%, and 220% strain, respectively). This may be because a higher crosslinking concentration results in more interactions between the polymer chains to prevent them from sliding over each other. Similarly, figure 1(b) shows that the ultimate strains decrease from ∼300% to 50% with the DCP concentration increasing from 2% to 8% at 70 °C. On the other hand, the cPEVA samples exhibit reduced mechanical properties at 70 °C compared to the room temperature. For example, the Young's Modulus is reduced to ∼3.3 MPa, and the yielding points (∼0.45 MPa) become less clear. For the sample with the same DCP concentration, the stiffness and stretchability are also reduced at a higher temperature. The reason may be twofold. On the one hand, the chain mobility becomes larger at higher temperature, resulting in easier deformation. On the other hand, the melting of the crystalline phase can also lead to lower stiffness and strength. Furthermore, the stress distribution in the sample can become less uniform due to the melting of the crystalline phase. Hereby, local cracks and defects can be more easily generated, which can result in lower stretchability.

Figure 2(a) presents the typical DSC curves of the 6% DCP sample based on three heating/cooling cycles. There are minimal changes in the melting temperatures, indicating high thermal repeatability and stability of cPEVA. Figure 2(b) illustrates the DSC curves of the cPEVA samples with different concentrations. It can be noted that increasing the DCP concentration shifts the melting point to a lower temperature. Gao *et al* [13] reported that the crosslinker concentration can significantly affect the crystallinity of cPEVA which dominates the melting and consolidating behavior. Hereby, the shifting-down of the melting point in this work may be attributed to high crosslinker (e.g. DCP) concentration induced weakening the crystallinity of the cPEVA. The XRD profiles of the different samples are included in supporting information (SI).

The influence of the DCP concentration on the two-way shape recoverability of samples is also studied. The thermally induced shape memory behavior (e.g. opening and recovering) of the bended cPEVA samples is demonstrated in figures 3(a)–(d) and video 1. The shape programming process is discussed in SI. Here, the bended samples are heated in hot water at 75 °C and cooled in cold water at 25 °C. It can be found that both the 2% and 6% DCP samples tend to open when dipped in the hot water bath and recover to bended shape when cooled. Notably, internal stresses are only stored in the folded area (e.g. the creases), which is opposed to the sample programmed by tensile force with uniformly stored stresses [31]. Tensile stresses are stored in the outer surface in the folded area, while compression stresses are stored in the inner surface. Hereby, upon heating, the outer surface tends to contract, and the inner surface tends to expand, so the bended shape tends to open, and vice versa. However, the 6% DCP sample shows a nearly complete recovery with a fast response, while the deformation of the 2% DCP sample cannot be fully recovered in even longer cooling time. The measured shape recovery ratio as a function of cooling time is displayed in figure 3(e). It is obviously observed that the 6% DCP sample can fully recover within 2 s, while the 2% DCP sample only has around 60% shape recovery ratio after 4 s (the recovery ratio is the ratio between the recovered angle after fully cooled and the opening angle when heated). This means that the 6% DCP sample exhibits relatively higher recovery speed and shape recoverability compared to 2% DCP sample. It is concluded that the shape memory behavior of cPEVA in our work is highly dependent on the DCP concentration.

As mentioned, increasing DCP concentration can enhance the two-way shape memory effect in terms of the response time and shape recoverability (see figure 3(e)). However, correspondingly, the mechanical properties (especially strength at high temperature) will be significantly compromised (see figure 1). Further increasing the DCP concentration leads to the sample fracture during the programming process at a high temperature (e.g. 95 °C). Hereby, 6% could be the optimal DCP concentration for the tradeoff between the mechanical and shape memory properties. The recoverable angle of the 6% DCP sample can be up to ∼40°, which is roughly three times

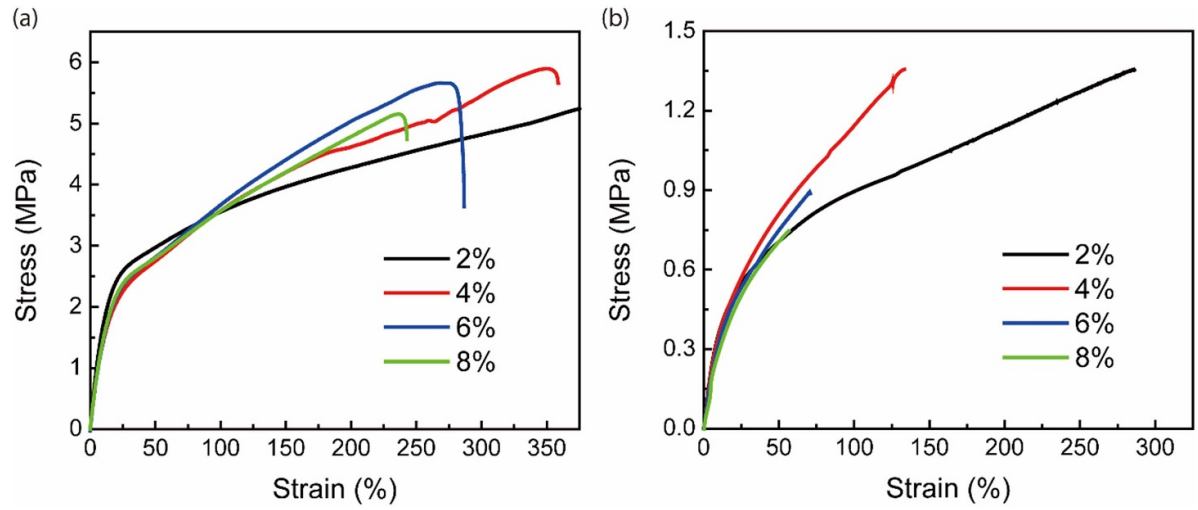

Figure 1. The stress–strain curves of the cPEVA samples with different DCP concentrations at (a) room temperature and (b) 70 °C.

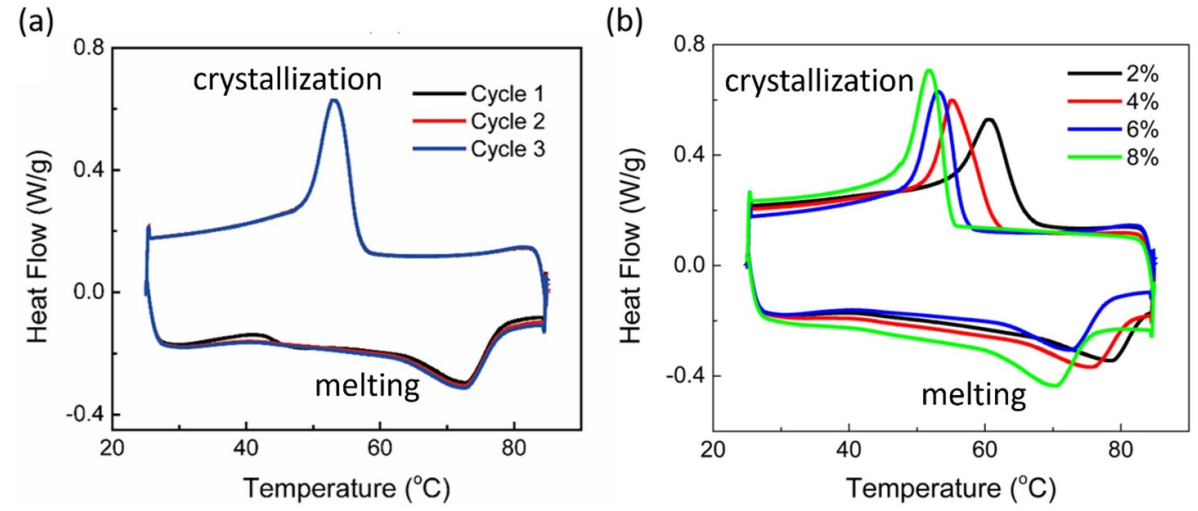

Figure 2. (a) Three DSC cycles of the 6% DCP sample (black, cycle 1; red, cycle 2; blue, cycle 3). (b) The DSC curves of the cPEVA samples with different DCP concentrations.

larger than the previous study by Gao *et al* [13]. Furthermore, video 2 shows that the two-way shape memory effect of the 6% DCP sample is still well maintained undergoing successive heating/cooling cycles. This indicates that the as-synthesized cPEVA sample possesses high thermo-mechanical stability.

The shape memory effect of cPEVA samples with multiple shapes (e.g. spiral in figure 3(f) and screw shape in figure 3(g)) has also been successfully proved. Video 3 and figure 3(f) exhibit that the spiral shape has an approximately 90° overall shape recovery. The two-way shape memory property of the screw shape is demonstrated in video 4 and figure 3(g). It can be seen that the end of the sample in the screw shape can spin freely and recover for more than one revolutions driven by the temperature. This indicates that the cPEVA samples own good designing versatility in terms of their programmable architectures, which may benefit the related applications in soft actuators performing complex motions. Soft actuators based on 6% DCP sample are fabricated to further demonstrate the designing versatility of as-synthesized cPEVA.

Gripping is accomplished by the cPEVA due to the two-way shape memory effect. As shown in figure 4(a), instead of directly using a bended cPEVA as the actuator, a curved cPEVA soft gripper with teeth assisting gripping has been fabricated which is inspired by a Venus flytrap. Unlike the bended sample, of which actuation zone is only the crease area, the curved sample has larger actuation zone, which provides larger opening gap and enables gripping larger volume of objects. Figure 4(b) and video 5 display the closure process of the cPEVA gripper initiated by natural cooling in air. Here, the gripper gradually closes in air followed by opening upon heating in 75 °C water. The reason may be that the outer surface will tend to expand due to internal tensile stress during cooling, while the inner surface will contract with internal compression stress, and vice versa. Notably, the closure speed of cPEVA gripper in air (lower cooling rate) is much slower than the responsive speed of bending/opening in hot/cold water bath (higher cooling rate). This means that the cPEVA is actuated by temperature difference instead of the heating/cooling rate.

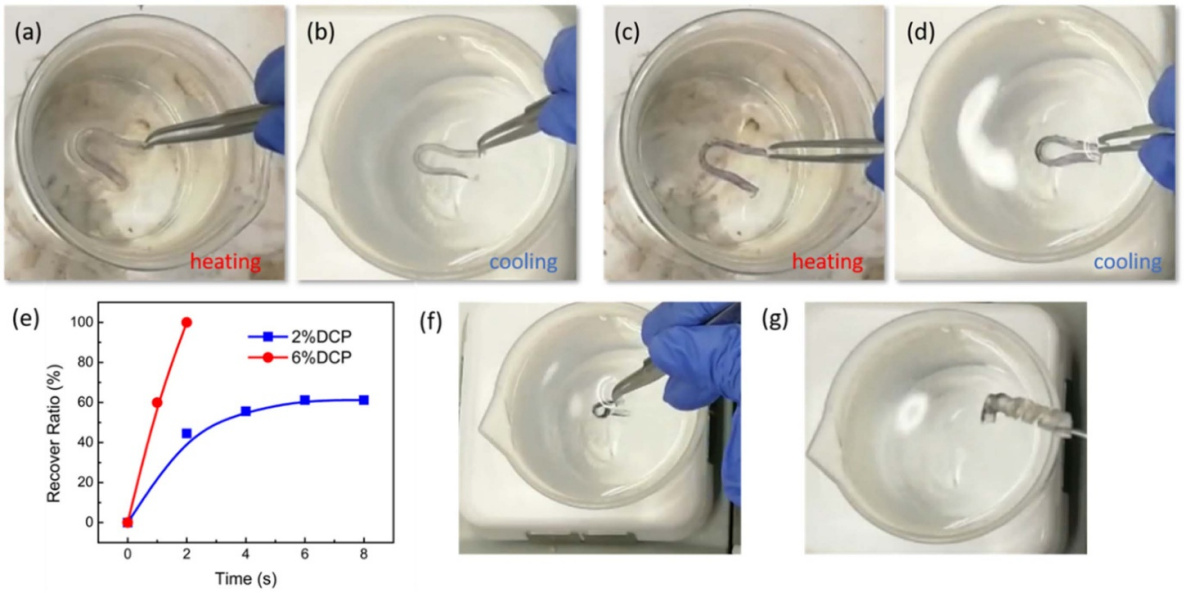

Figure 3. The digital images of the two-way shape memory effect of the bended 2% ((a), heating; (b), cooling) and 6% ((c), heating; (d), cooling) DCP samples. (e) The shape recovery ratios of the 2% and 6% DCP samples as a function of cooling time. Digital images of the (f) spiral and (g) screw shape of 6% DCP sample.

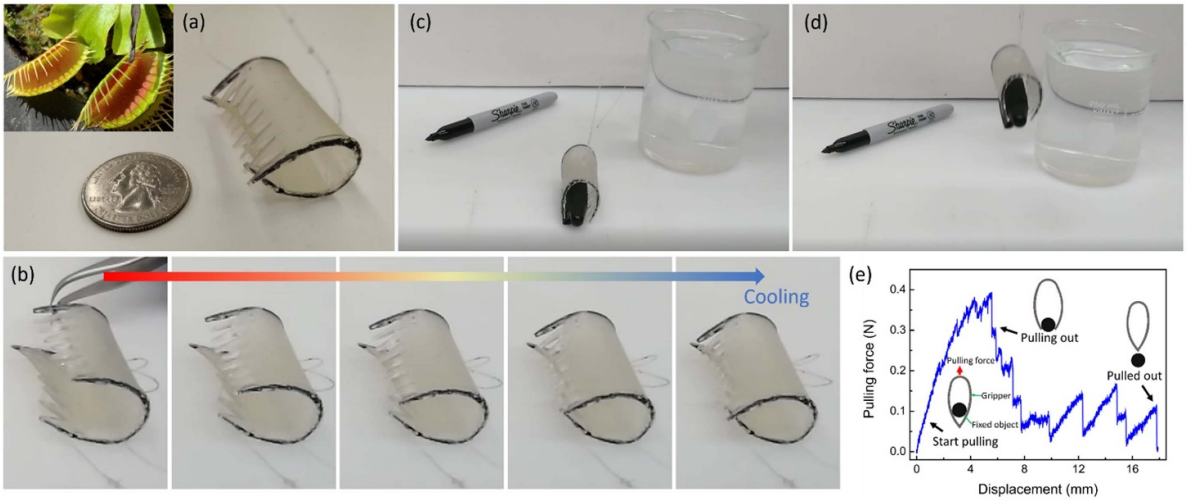

Figure 4. (a) The digital image of the cPEVA gripper, where the inset shows the optical image of the Venus flytrap. (b) The process of the cPEVA gripper closure when cooling naturally in air. Grasping (c) and lifting (d) of a marker pen cap. (e) The pulling force of the gripper with a fixed solid cylinder.

However, the response speed is significantly dependent on the heating/cooling rate. As shown in figure 4(b), the cPEVA gripper can completely return to its original shape when fully cooled. Figures 4(c), (d) and video 6 show that the cPEVA gripper is able to grasp a regular marker cap. Notably, the mass of the marker cap is 2.0 g, while the mass of the gripper is only 2.1 g, which means the gripper can generate the grasping load as large as its own weight. This indicates that the large output forces of this cPEVA gripper enables the corresponding soft actuators and robots adapting to complex systems requiring high load capacity, which may be advantageous over other two-way SMPs, such as liquid crystals. Figure 4(e) shows the pulling force of the gripper with a fixed solid cylinder with diameter 10 mm, and it is measured by an Instron testing machine with 1 mm min^{-1} pulling speed. Prior to testing, the gripper is fully closed, and the fixed cylinder is fully encapsulated in the gripper. The pulling force increases rapidly until about 0.4 N in the beginning, and then starts to decrease when the cylinder is partially pulled out. When more than half of the cylinder is pulled out, some local friction and sliding between the cylinder and the teeth of the gripper are generated, which corresponds to the zigzag shape in the pulling force diagram. The pulling force is comparable with the gripper developed by Wang *et al* [32], although the design in this work is simpler.

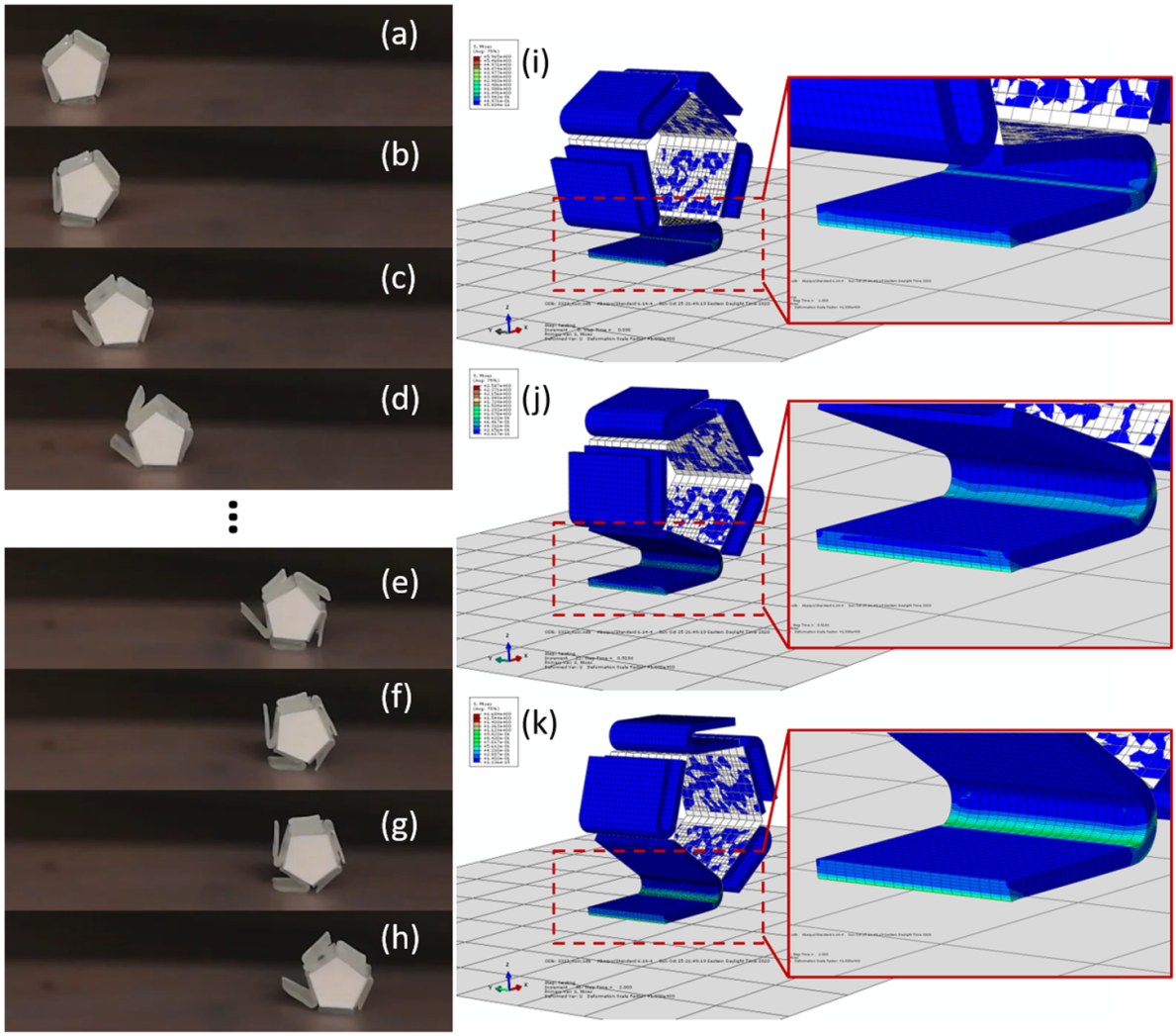

Figure 5. The first several steps of the pentagon sample self-rolling on a 90 °C hot surface (a)–(d). The pentagon sample cools down in air (e) and (f). The sample is reheated again (g). The second self-rolling cycle initiates (h). One single self-rolling step is simulated with finite element method (i)–(k).

Walking is another mainstream locomotion for soft robotics. Here, we present a walking strategy by a self-rolling design based on the two-way shape memory effect. A cPEVA self-rolling structure in a pentagon shape (1.7 cm in edge length and 2 cm in depth) is manufactured with the 6% DCP sample (see figure S4(a)). The self-rolling pentagon structure can indicate the output torque magnitude. On the other hand, it is also a basic concept which can be further expanded with more sophisticated structures [33]. The pentagon frame is made by regular cardboard, and each side has a bended cPEVA serving as the actuators. The total mass of the structure is 5 g while each cPEVA is around 0.74 g. The self-rolling process is visually demonstrated in figures 5(a)–(h) and video 7. In this work, the structure is rolling on a hot surface with 90 °C. Notably, the structure is able to roll for more than one revolutions as shown in figures 5(a)–(h) and video 7.

For the first rolling step, the 1st cPEVA actuator that closely contacts the hot surface will be heated, leading to the cPEVA opening. As shown in figures 5(a) and (b), the first rolling step is initiated by the cPEVA actuator opening. As shown in figures 5(c) and (d), when the opening angle of the 1st cPEVA is large enough to lift the self-rolling structure to an unbalanced state, the structure will roll one step forward. Subsequently, the next (2nd) cPEVA actuator contacts the hot surface and is actuated by heating. In the meantime, the previous (1st) cPEVA actuator detaches from the hot surface, which causes shape recovery (cPEVA folding) due to cooling. In this manner, the structure realizes self-rolling on the surface step by step driven by the temperature changes. Notably, for each step, the minimum required moment to lift the pentagon should be larger than that generated by the weight of the structure, which can be easily obtained as:

$$M = \frac{W}{2\cos 54^\circ} \cdot a \cdot \sin\left(36^\circ - \alpha\right)$$

where the W is the weight of the structure, a is the length of each side, and α is the lifting angle (0°–36°, illustrated in figure S4(b)). The relationship between M and α is further demonstrated in figure S4(c). It can be seen that the required moment is nearly linear decreasing with the lifting angle. It

can also be easily concluded that the maximum required lifting angle is 36°, which is smaller than the abovementioned maximum recover angle of the cPEVA synthesized in this work.

Nonetheless, in order to initiate the second self-rolling revolution period, it is necessary to cool down the hot surface. As abovementioned, the cooling rate of cPEVA is relatively low in air. Therefore, the hot surface should be cooled when the 5th cPEVA actuator starts to contact the surface, as shown in figure 5(e). In this way, as shown in figures 5(f) and (g), the subsequent (1st) cPEVA can be gradually cooled and recovers back to its initial bended shape. Then the surface is heated up to 90 °C again, and the second self-rolling revolution period is initiated. Figure 5(h) displays the first self-rolling step in the second revolution period. Consequently, the structure can move forward step by step by iterating the previous process.

To investigate and understand the mechanisms of the self-rolling, a simulation with finite element analysis is conducted. The simulation model is illustrated in figure S4(d). The simulation is implemented by a commercial finite element software Abaqus (version 6.14, Dassault Systems Simulia Corp., USA). The constitutive model we used in this study is designed for semi-crystalline SMPs. Semi-crystalline SMPs have both crystalline region and rubbery region. The constitutive model involves four steps, the loading (rubbery phase), cooling (phase transition), unloading (semi-crystalline phase) and heating (phase transition) of the polymer. Each step is governing by a stress function which is associated with storage modulus and loss modulus. Related details can be found in our previous study which provides a typical constitutive model for SMPs in the finite element simulation [34]. Figures S4(e) and (f) show the input properties of materials including the storage modulus, loss modulus, and tan delta sweeping with temperatures for the simulation. The DMA properties are measured with 6% DCP sample at 10 Hz. The results correspond well with the previous study by Wang *et al* [30]. Figures 5(i)–(k) and video 8 show the self-rolling process simulated by the finite element method. It is notable that the cPEVA actuator starts to open when contacting the hot surface, which resembles the experimental results. Furthermore, the internal stresses are generated, which is attributed to the shape recovery. As the temperature increases, the internal stresses start to gradually propagate up in the hinge area, corresponding to the heat transfer direction. Therefore, it can be speculated that the localized internal stresses inspired by heating serve as the driven force for the cPEVA opening. As shown in figure S4(g), when the center of the pentagon surpasses the reference line (dashed), the structure will roll one step forward due to the loss of balance. In summary, the self-rolling structure made by cPEVA indicates that the cPEVA is able to produce large output force and recover shape from large deformation. This study may provide important insights in preparing smart materials for advanced soft actuator applications.

The soft actuators need to fast release a certain amount of energy to accomplish jumping process. Here, we present a strategy for jumping with the as-synthesized cPEVA samples. Figures 6(a)–(d) and video 9 exhibit the sample jumping process. Figure 6(e) further demonstrates the sample jumping mechanism. The whole process can be divided into three

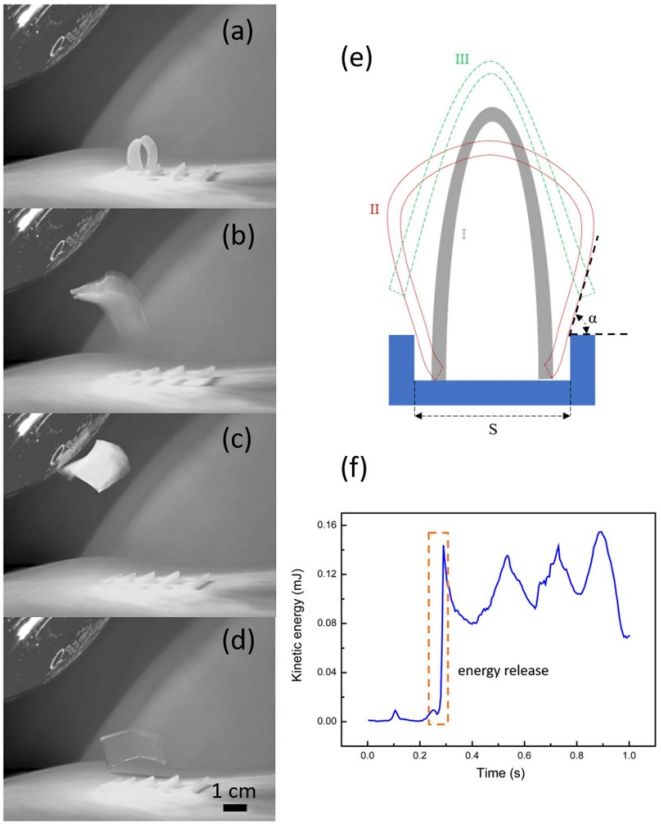

Figure 6. (a)–(d) The jumping process of the cPEVA sample. (e) The schematic of the recovering and jumping of the cPEVA. (f) The kinetic energy diagram of the jumping process.

stages. For stage I, the bended cPEVA sample is initially vertically placed in a 3D printed holder. The sample starts to recover when it is heated by light with an infrared higher. For stage II, the local curvature of the crease area will be decreased. When the two legs of the cPEVA samples are clamped by the two blockers on the holder, the vicinity of the initial crease area will tend to swell into a curved surface, which is shown in figure 6(a). In this way, an elastic energy barrier is created. For stage III, when the stored energy is large enough, the two legs will slip upwards, and the sample can jump from the holder for ∼5 cm with a large energy release (figures 6(b)–(d)). Figure 6(F) shows the kinetic energy evolution of this structure which is calculated by finite element simulation. It can be found that there is a kinetic energy jump within a very small time period, which is due to the stored energy passes the energy barrier and fast releases. Notably, the jumping process can be influenced by the ratio of the sample length and the spacing between the two blockers on the holder s. It is found that when the s is larger than 10 mm (sample length 30 mm), the cPEVA sample cannot jump off from the holder. The possible reason is that the contacting angle between the leg and the blocker α will be larger than 90° when $s \geqslant 10$ mm. In this way, the sample will be clamped by the holder and cannot slip upward. Video 9 shows that the sample can jump up when the $s = 5$ and 7.5 mm, and the cPEVA sample can only gradually recover to the permanent shape without the jumping when there is no fast energy release.

4. Conclusions

In this study, a crosslinked PEVA-based two-way SMP has been successfully synthesized by using DCP as the crosslinker. The effect of the DCP concentration on the mechanical properties and the two-way shape memory properties has been systematically studied. Our results show that increasing DCP concentration can enhance the shape memory effect but weakens the mechanical properties. Finally, the 6% DCP cPEVA with high responsive speed and shape recoverability is found to be the ideal material for the fabrication of soft actuators. Three locomotion in the form of a gripping, a self-rolling, and jumping are accomplished by the as-synthesized cPEVA. Our experiments on these strategies show the efficiency of this polymer in producing large output forces in a Venus flytrap-inspired actuator, making a self-rolling pentagon-shaped robot, and accomplishing jumping to perform complex motions. Finite element simulations are also conducted to investigate the mechanisms that control the self-rolling and jumping behaviors. It is found that the realization of self-rolling is due to the internal stress propagation and the jumping is due to fast energy release which are activated by temperature-induced shape memory behavior. This provides critical insights into the design of smart materials for the potential soft actuator applications.

Data availability statement

The data that support the findings of this study are available upon reasonable request from the authors.

Acknowledgment

Financial support from the NSF CMMI Grant 2016474 is gratefully acknowledged.

ORCID iDs

Shima Shahab https://orcid.org/0000-0003-1970-5345
Reza Mirzaeifar https://orcid.org/0000-0003-3427-0714

References

[1] El-Atab N, Mishra R B, Al-Modaf F, Joharji L, Alsharif A A, Alamoudi H, Diaz M, Qaiser N and Hussain M M 2020 Soft actuators for soft robotic applications: a review *Adv. Intell. Syst.* **2** 2000128
[2] Boyraz P, Runge G and Raatz A 2018 An overview of novel actuators for soft robotics *Actuators* **7** 48
[3] Xing S-T, Wang P-P, Liu S-Q, Xu Y-H, Zheng R-M, Deng Z-F, Peng Z-F, Li J-Y, Wu Y-Y and Liu L 2020 A shape-memory soft actuator integrated with reversible electric/moisture actuating and strain sensing *Compos. Sci. Technol.* **193** 108133
[4] Kang T-H, Lee J-M, Yu W-R, Youk J H and Ryu H W 2012 Two-way actuation behavior of shape memory polymer/elastomer core/shell composites *Smart Mater. Struct.* **21** 035028
[5] Peng K, Zhao Y, Shahab S and Mirzaeifar R 2020 Ductile shape-memory polymer composite with enhanced shape recovery ability *ACS Appl. Mater. Interfaces* **12** 58295–300
[6] Chen S, Hu J, Zhuo H and Zhu Y 2008 Two-way shape memory effect in polymer laminates *Mater. Lett.* **62** 4088–90
[7] Ware T H, McConney M E, Wie J J, Tondiglia V P and White T J 2015 Voxelated liquid crystal elastomers *Science* **347** 982
[8] Shahsavan H, Aghakhani A, Zeng H, Guo Y, Davidson Z S, Priimagi A and Sitti M 2020 Bioinspired underwater locomotion of light-driven liquid crystal gels *Proc. Natl Acad. Sci.* **117** 5125
[9] Thomsen D L, Keller P, Naciri J, Pink R, Jeon H, Shenoy D and Ratna B R 2001 Liquid crystal elastomers with mechanical properties of a muscle *Macromolecules* **34** 5868–75
[10] Tomić N Z, Međo B I, Stojanović D B, Radojević V J, Rakin M P, Jančić-Heinemann R M and Aleksić R R 2016 A rapid test to measure adhesion between optical fibers and ethylene–vinyl acetate copolymer (EVA) *Int. J. Adhes. Adhes.* **68** 341–50
[11] Osman A F, Hamid A R, Fitri T F, Fauzi A A and Halim K A 2020 Poly(ethylene-co-vinylacetate) copolymer based nanocomposites: a review *IOP Conf. Ser.: Mater. Sci. Eng.* **864** 012121
[12] Behl M, Kratz K, Noechel U, Sauter T and Lendlein A 2013 Temperature-memory polymer actuators *Proc. Natl Acad. Sci.* **110** 12555
[13] Gao Y, Liu W and Zhu S 2018 Reversible shape memory polymer from semicrystalline poly(ethylene-co-vinyl acetate) with dynamic covalent polymer networks *Macromolecules* **51** 8956–63
[14] Scalet G 2020 Two-way and multiple-way shape memory polymers for soft robotics: an overview *Actuators* **9** 10
[15] Ghosh P, Rao A and Srinivasa A R 2013 Design of multi-state and smart-bias components using shape memory alloy and shape memory polymer composites *Mater. Des.* **44** 164–71
[16] Westbrook K K, Mather P T, Parakh V, Dunn M L, Ge Q, Lee B M and Qi H J 2011 Two-way reversible shape memory effects in a free-standing polymer composite *Smart Mater. Struct.* **20** 065010
[17] Liu Y, Razzaq M Y, Rudolph T, Fang L, Kratz K and Lendlein A 2017 Two-level shape changes of polymeric microcuboids prepared from crystallizable copolymer networks *Macromolecules* **50** 2518–27
[18] Yang Q, Fan J and Li G 2016 Artificial muscles made of chiral two-way shape memory polymer fibers *Appl. Phys. Lett.* **109** 183701
[19] Hui J, Xia H, Fu Y, Qiu Y and Ni Q-Q 2020 Two-way reversible shape memory properties of benzoyl peroxide crosslinked poly(ethylene-co-vinyl acetate) under different stress conditions *Macromol. Mater. Eng.* **305** 1900825
[20] Acome E, Mitchell S K, Morrissey T G, Emmett M B, Benjamin C, King M, Radakovitz M and Keplinger C 2018 Hydraulically amplified self-healing electrostatic actuators with muscle-like performance *Science* **359** 61
[21] Chi Y, Tang Y, Liu H and Yin J 2020 Leveraging monostable and bistable pre-curved bilayer actuators for high-performance multitask soft robots *Adv. Mater. Technol.* **5** 2000370
[22] Tang Y, Zhang Q, Lin G and Yin J 2018 Switchable adhesion actuator for amphibious climbing soft robot *Soft Robot.* **5** 592–600
[23] Tang Y, Chi Y, Sun J, Huang T-H, Maghsoudi O H, Spence A, Zhao J, Su H and Yin J 2020 Leveraging elastic instabilities for amplified performance: spine-inspired high-speed and high-force soft robots *Sci. Adv.* **6** eaaz6912

[24] Chen T, Bilal O R, Shea K and Daraio C 2018 Harnessing bistability for directional propulsion of soft, untethered robots *Proc. Natl Acad. Sci.* **115** 5698
[25] Ma K Y, Chirarattananon P, Fuller S B and Wood R J 2013 Controlled flight of a biologically inspired, insect-scale robot *Science* **340** 603
[26] Koh J-S, Yang E, Jung G-P, Jung S-P, Son J H, Lee S-I, Jablonski P G, Wood R J, Kim H-Y and Cho K-J 2015 Jumping on water: surface tension–dominated jumping of water striders and robotic insects *Science* **349** 517
[27] Zhakypov Z, Mori K, Hosoda K and Paik J 2019 Designing minimal and scalable insect-inspired multi-locomotion millirobots *Nature* **571** 381–6
[28] Tang Y, Li Y, Hong Y, Yang S and Yin J 2019 Programmable active kirigami metasheets with more freedom of actuation *Proc. Natl Acad. Sci.* **116** 26407
[29] Jiang Y, Korpas L M and Raney J R 2019 Bifurcation-based embodied logic and autonomous actuation *Nat. Commun.* **10** 128
[30] Wang K and Deng Q 2019 The thermal and mechanical properties of poly(ethylene-co-vinyl acetate) random copolymers (PEVA) and its covalently crosslinked analogues (cPEVA) *Polymers* **11** 1055
[31] Yan C, Yang Q and Li G 2020 A phenomenological constitutive model for semicrystalline two-way shape memory polymers *Int. J. Mech. Sci.* **177** 105552
[32] Wang W, Yu C Y, Abrego Serrano P A and Ahn S-H 2019 Soft grasping mechanisms composed of shape memory polymer based self-bending units *Composites* B **164** 198–204
[33] Kotikian A, McMahan C, Davidson E C, Muhammad J M, Weeks R D, Daraio C and Lewis J A 2019 Untethered soft robotic matter with passive control of shape morphing and propulsion *Sci. Robot.* **4** eaax7044
[34] Bhargava A, Peng K, Stieg J, Mirzaeifar R and Shahab S 2017 Focused ultrasound actuation of shape memory polymers; acoustic-thermoelastic modeling and testing *RSC Adv.* **7** 45452–69